

Research Article

#Joint first authorship

SOA is now associated with Clinical Laboratory Sciences Department, Faculty of Applied Medical Sciences, Umm Al-Qura University

Cite this article: Caygill CH *et al.* (2025) An accessible 3D HepG2/C3A liver spheroid model supporting the complete intrahepatocytic lifecycle of *Plasmodium falciparum*. *Parasitology*, 1–8. <https://doi.org/10.1017/S0031182025100322>

Received: 13 January 2025
Revised: 24 April 2025
Accepted: 24 April 2025

Keywords:



HepG2/C3A; malaria; *Plasmodium*; spheroids

Corresponding author: Claire H. Caygill;
Email: claire.caygill@lstm.ac.uk

© Liverpool School of Tropical Medicine, 2025. Published by Cambridge University Press. This is an Open Access article, distributed under the terms of the Creative Commons Attribution licence (<http://creativecommons.org/licenses/by/4.0>), which permits unrestricted re-use, distribution and reproduction, provided the original article is properly cited.



An accessible 3D HepG2/C3A liver spheroid model supporting the complete intrahepatocytic lifecycle of *Plasmodium falciparum*

Claire H. Caygill^{1, #} , Salwa Omar Alqurashi^{1, #}, Adriana Adolff¹, Jessica Carson¹, Angelika Sturm², Daniel S. Evans¹, Jess B. Jinks¹, Koen J. Dechering², Lisa Reimer¹, Shaun H. Pennington¹, Parveen Sharma³, Stephen A. Ward¹ and Giancarlo A. Biagini^{1, #} 

¹Centre for Drugs and Diagnostics, Department of Tropical Disease Biology, Liverpool School of Tropical Medicine, Pembroke Place L3 5QA, UK; ²TropiQ Health Sciences, Nijmegen, The Netherlands and ³Department of Cardiovascular & Metabolic Medicine and Liverpool Centre for Cardiovascular Sciences, Institute of Life Course and Medical Sciences, University of Liverpool, Liverpool, Merseyside, UK

Abstract

Current liver-stage *Plasmodium falciparum* models are complex, expensive and largely inaccessible, hindering research progress. Here, we show that a 3D liver spheroid model grown from immortalized HepG2/C3A cells supports the complete intrahepatocytic lifecycle of *P. falciparum*. Our results demonstrate sporozoite infection, development of exoerythrocytic forms and breakthrough infection into erythrocytes. The 3D-grown spheroid hepatocytes are structurally and functionally polarized, displaying enhanced albumin and urea production and increased expression of key metabolic enzymes, mimicking *in vivo* conditions – relative to 2D cultures. This accessible, reproducible model lowers barriers to malaria research, promoting advancements in fundamental biology and translational research.

Introduction

Malaria continues to be a global health emergency. Despite intensive efforts, the WHO's 2023 World Malaria Report estimated that the number of global malaria cases in 2022 remains stubbornly high at 249 million, exceeding pre-COVID-19 pandemic levels in 2019 (World malaria report, 2023).

Chemotherapy continues to be a cornerstone to the multifaceted approach for malaria control and elimination and whilst the past 2 decades has delivered a robust pipeline of promising candidate drugs and several new treatments that act on the asexual blood stages (categorized as target candidate profile 1 [TCP-1]), there has been little progress in the development of effective therapies active against liver-stage hypnozoites (*Plasmodium vivax* and *P. ovale*) or hepatic *P. falciparum* schizonts (TCP-3 and TCP-4, respectively) (Siqueira-Neto *et al.*, 2023).

The establishment of a stable *in vitro* culture system for the asexual blood stages of *P. falciparum* (Trager and Jensen, 1976) has been vital in unlocking our understanding of the intraerythrocytic stages of malaria infection and in advancing antimalarial drug discovery efforts for malaria treatment (TCP-1). Conversely, the relative paucity in our understanding of the biology of the hepatic stage of development and limited TCP3/4 pipeline has, in part, been attributed to the difficulty of establishing *in vitro* human liver stage malaria models, with current methods deemed expensive, laborious and impractical (Siqueira-Neto *et al.*, 2023).

Initial studies attempting to establish stable *in vitro* models of malaria life stages using immortalized hepatoma cell lines, such as HepG2, HSS-102 and HC-04, achieved limited success and were unable to demonstrate breakthrough infection into erythrocytes. While these human hepatoma cell lines, allowed partial development of *Plasmodium* parasites, significant limitations persisted. For instance, HepG2-A16 cells could support sporozoite invasion but failed to sustain full parasite development. Similarly, HC-04 cells, though capable of supporting the liver stages of *P. falciparum* and *P. vivax*, exhibited reduced parasite viability and did not facilitate merozoite egress into erythrocytes due to their limited culture lifespan (Chattopadhyay *et al.*, 2010; Tweedell *et al.*, 2019; Valenciano *et al.*, 2022).

More sophisticated approaches have achieved greater success in developing *in vitro* models for malaria research. Techniques such as using induced pluripotent stem cell-derived hepatocyte-like cells, immortalized hepatocyte-like cell lines, co-culture systems, 2D primary

human hepatocyte monolayer systems and 3D cell cultures have shown considerable promise (Valenciano *et al.*, 2022). These advanced models have allowed large-scale drug screening campaigns (Roth *et al.*, 2018; Maher *et al.*, 2021) and have improved our understanding of *Plasmodium* liver stage biology. However, challenges remain, including limited expression of drug metabolism enzymes, difficulty in maintaining cultures long-term and low sporozoite infection rates. Additionally, these advanced technologies are not widely accessible, particularly to laboratories in malaria-endemic low- and middle-income countries that often face resource and capability constraints. This disparity highlights the need for more accessible and robust *in vitro* models to support global malaria research efforts.

Multiple studies have shown that immortalized hepatocarcinoma cell lines cultured in 3D have superior liver-specific functionality when compared to monolayer cultures (Cox *et al.*, 2020). A simple, high-throughput method of generating 3D cultures is through the creation of 'spheroids'. Unlike more complicated 3D cell culture techniques, spheroids are simple to generate, inexpensive to culture, reproducible and may be analysed using a variety of methods (Cox *et al.*, 2020).

HepG2/C3A cells are a derivative of the HepG2 cell line and have been shown to display greater contact inhibition and higher levels of liver-specific proteins and metabolic enzymes (Štampar *et al.*, 2020; Kelly, JH US Patent 5290684, 1990). Here, we investigated whether a previously reported method of generating 3D liver spheroids from the immortalized HepG2/C3A cell line which demonstrated *in vivo*-like morphology and phenotype (Gaskell *et al.*, 2016; Štampar *et al.*, 2020) could be used to support the complete intrahepatocytic lifecycle of *Plasmodium*. Data are presented demonstrating that the HepG2/C3A liver spheroid model supports initial *P. falciparum* sporozoite infection, the development of exo-erythrocytic forms, and the subsequent egress of merozoites and breakthrough infection of erythrocytes. These data are discussed in the context of a method that is reproducible, inexpensive and accessible.

Materials and methods

HepG2/C3A 2D cell culture

HepG2/C3A cells were maintained in EMEM (LGC standards, Middlesex, UK), supplemented with 10% FBS (Sigma, UK) and 1% penicillin/streptomycin (Fisher Scientific, UK) at 37 °C with 5% CO₂. Cell culture medium was replaced every 3–4 days and cells were not allowed to exceed 80% confluency. Upon reaching 80% confluence, HepG2/C3A cells were washed once with PBS and incubated 0.25% (w/v) Trypsin EDTA (Fisher Scientific, UK) for 5 min at 37 °C to detach the cells from the flask. After 5 min, cell culture media was added and centrifuged at 173 × g for 5 min. Supernatant was then removed, remaining pellet resuspended in cell culture media and cell number counted with haemocytometer. HepG2/C3A cells were then seeded into fresh flasks at a seeding density of 2 × 10⁵ cells mL⁻¹. For albumin and urea comparative studies to 3D spheroids, HepG2/C3A cells were seeded 1000 cells per well (matching spheroid seeding density, described below) in 96-well cell culture plates in cell culture media and incubated at 37 °C with 5% CO₂ for 20 days.

HepG2/C3A spheroid formation and growth

HepG2/C3A spheroids were grown using the liquid overlay technique, described elsewhere (Delves *et al.*, 2016; Gaskell *et al.*, 2016).

In brief, 100 µL of sterile 1.5% agarose in EMEM was added per well to flat bottom 96-well cell culture plates. Plates were then allowed to cool and solidify for 3 h before and stored at 4 °C upside down to prevent condensation for up to 1 month. Agarose plates were pre-warmed to 37 °C and HepG2/C3A cells were seeded at 1000 cells per well in 100 µL EMEM. Seeded plates were then centrifuged at 173 × g for 5 min and incubated for 72 h at 37 °C with 5% CO₂ to allow formation of spheroids. Media changes were conducted every 2–3 days. Spheroid growth was monitored for 21 days and representative images taken using Echo Revolve R4 microscope with 20× objective. Images were analysed using ImageJ software to obtain spheroid diameter.

Quantification of protein, albumin and urea production

Cell lysates were obtained by disrupting 2D monolayer cultures and HepG2/C3A spheroid cultures on days 5, 9, 12, 14 and 21 using lysis buffer (250 mM sucrose, 50 mM Tris-HCl pH7.4, 5 mM MgCl₂, 1 mM β-mercaptoethanol and 1% Triton X-100) and stored at –80 °C. Protein concentrations from spheroid and monolayer cell lysates were quantified using Bio-Rad Protein Assay (Bio-Rad Laboratories), according to the manufacturer's instructions.

Supernatants for spheroid and 2D cultures were also collected on days 4, 8, 12, 16 and 20 and stored at –80 °C until required for quantification of albumin and urea. Albumin and urea were quantified using the Albumin Human ELISA Kit (Abcam) and the Urea Assay Kit (Abcam), respectively, according to manufacturer's instructions. Albumin and urea data were normalized to total 2D or 3D spheroid protein content, as measured by Bio-Rad Protein Assay, described above.

Measurement of CYP3A4 and CYP2D6 activity

CYP3A4 and CYP2D6 activity was measured using P450-GLO assay (Promega) on day 4 of 2D and 3D HepG2/C3A cultures, according to manufacturer's instructions. Data were normalized based on the viable cell mass of day 4 2D and 3D spheroid cultures to account for any differences between cultures. This was measured by CellTitre-Glo Luminescent Cell Viability Assay (Promega), according to the manufacturer's instructions. In brief, CellTitre-Glo reagent was added to 2D and 3D cultures, followed by mixing on an orbital shaker for 2 min to induce cell lysis and then incubated for 15 min at room temperature. Luminescence was then measured using POLARstar OMEGA plate reader (BMG Labtech).

Immunofluorescence analysis of spheroids

Spheroids were fixed with 4% paraformaldehyde for 1 h at 4 °C, washed 3 times with PBS and permeabilized with 0.5% Triton X-100 in Tris-Buffered Saline with 0.05% Tween20 (TBST) overnight at 4 °C. Spheroids were then blocked with 0.1% Triton X-100/5% BSA in TBST for 2 h at room temperature. Primary antibodies monoclonal antibody 7.2 anti-GAPDH (1:100, obtained from The European Malaria Reagent Repository [<http://www.malariaresearch.eu>]), rabbit anti-HSP70 (*P. falciparum*) polyclonal (1:200, StressMarq Biosciences Inc., SPC-186D) or rabbit recombinant monoclonal multidrug resistance-associated protein 2 (MRP2) antibody (1:200, Abcam, ab172630) were diluted in 0.1% Triton X-100/1% BSA in TBST and incubated with spheroids overnight at 4 °C. Spheroids were washed 3 times with 0.1% Triton X-100 in TBST and incubated with Goat anti-Rabbit IgG (H + L) Cross-Adsorbed Secondary Antibody, Alexa Fluor™ 568

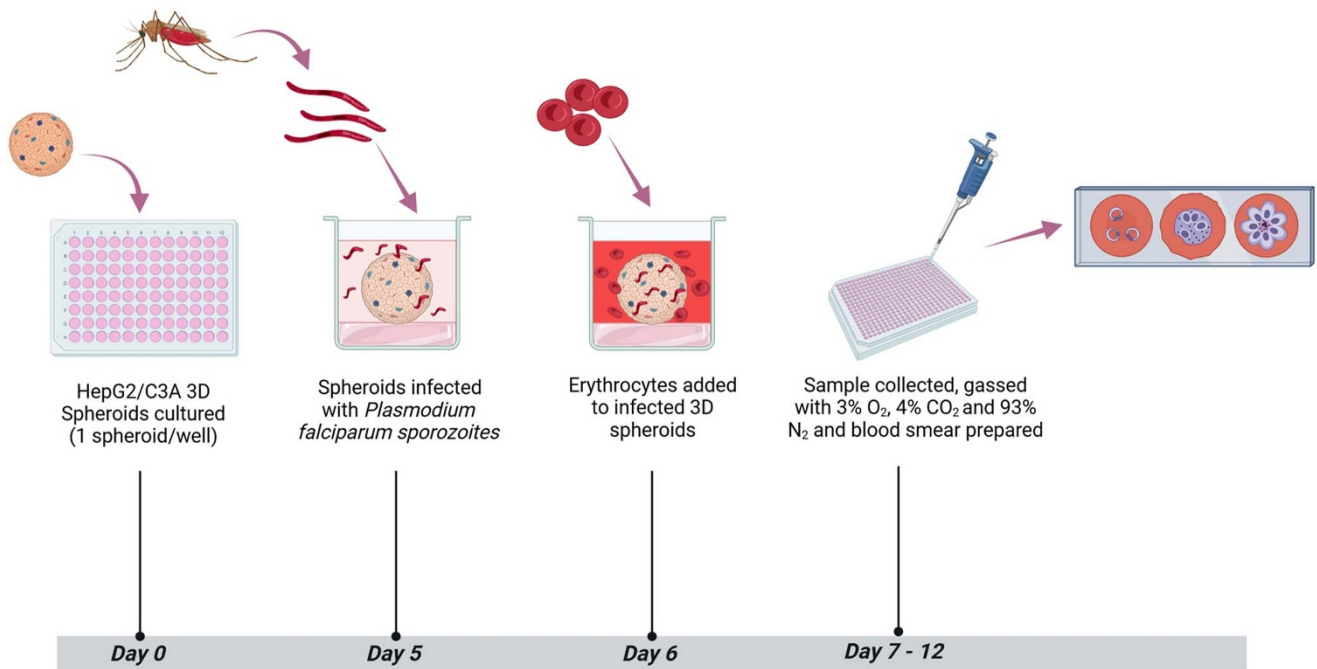


Figure 1. Schematic of HepG2/C3A 3D spheroid infection with *P. falciparum*, sample collection and assessment of blood-stage breakthrough timeline.

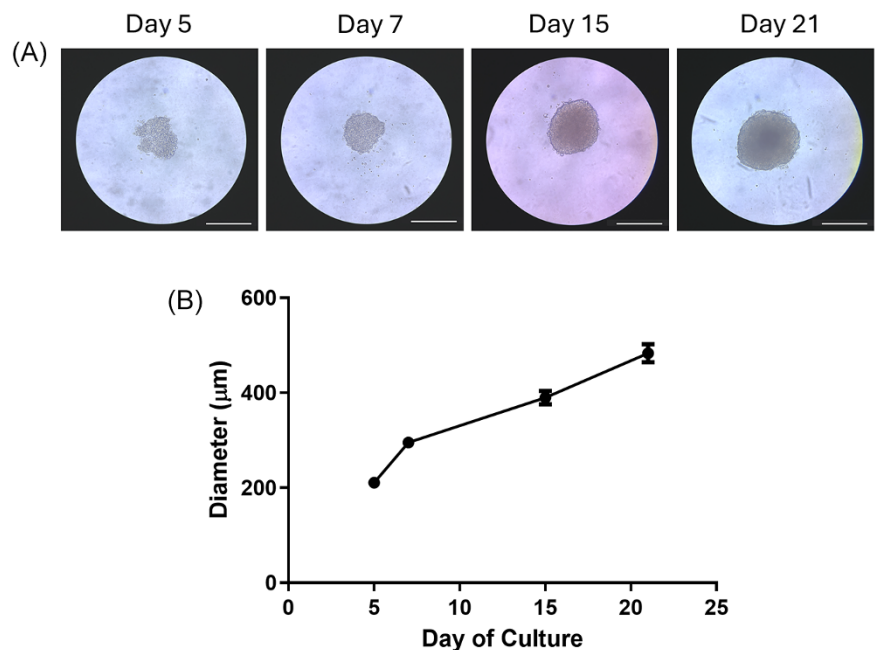


Figure 2. HepG2/C3A spheroid growth. HepG2/C3A cells were seeded at 1000 cells per well and incubated for 21 days to allow spheroid formation. Growth was observed and images acquired using Echo Revolve R4 microscope with 20× objective on days 5, 7, 15 and 21. Representative images are displayed, white scale bar represents 380 µm (A). Images were analysed using ImageJ software to obtain spheroid diameter (B). Data represent the mean ± SEM of $n = 3$ biological replicates, conducted in triplicate.

(1:1000, Thermo Fisher Scientific, A-11011), Goat anti-Mouse IgG (H + L) Cross-Adsorbed Secondary Antibody, Alexa Fluor™ 488 (1:1000, Thermo Fisher Scientific, A-11001), goat anti-Rabbit IgG (H + L) Cross-Adsorbed Secondary Antibody, Alexa Fluor 647 (1:1000, Thermo Fisher Scientific, A-21244) or Alexa Fluor 488 mouse monoclonal Anti-PGP9.5 (P-Glycoprotein 9.5 [Pg-P]) antibody (1:1000, Abcam, ab197733) in 0.1% Triton X-100/5% BSA in TBST and incubated overnight at 4 °C. DAPI, to detect cell nuclei (1:5000, Thermo Fisher Scientific, 62248), and/or phalloidin for detection of F-actin filaments (1:250, Thermo Fisher Scientific, A12380) in 0.1% Triton X-100/5% BSA in TBST was added to the

spheroids and incubated for 1 h at room temperature in the absence of light. Finally, spheroids were mounted with Prolong Gold (Life Technologies, P36930) onto a glass microscope slide with round, 13 mm coverslips (Agar Scientific Ltd, UK). Images were acquired at 40× objective using a Zeiss LSM880 confocal microscope and analysed with Zeiss Zen Blue software (Zeiss, Germany).

Statistical analyses

Multiple unpaired *t*-tests with Holm–Šidák correction for multiple comparisons and single unpaired *t*-tests were performed using

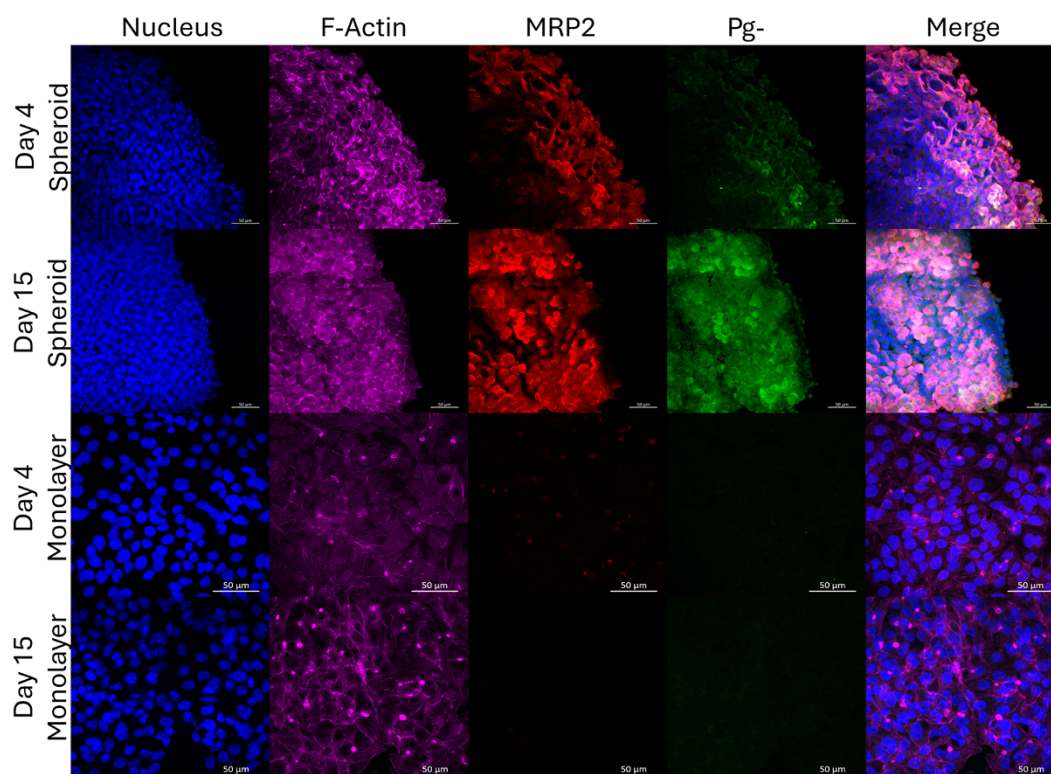


Figure 3. Hepatocyte transporters Pg-P and MRP2 expressed in HepG2/C3A 3D spheroids, but not in 2D culture. Secondary structures were visualized by immunofluorescence staining of HepG2/C3A 2D monolayer and 3D spheroid cultures on days 4 and 15. Phalloidin stain was used to visualize F-actin (purple) and canalicular transporters MRP2 (red) and Pg-P (green) were visualized with rabbit recombinant monoclonal MRP2 antibody (1:200, Abcam, ab172630), with goat anti-Rabbit IgG (H + L) Cross-Adsorbed Secondary Antibody, Alexa Fluor 647 (1:1000, Thermo Fisher Scientific, A-21244) and Alexa Fluor 488 mouse monoclonal Anti-pgp9.5 (Pg-P) antibody (1:1000, Abcam, ab197733), respectively. HepG2/C3A nuclei were stained with DAPI (blue). Representative images are shown of $n = 3$ biological replicates, images were taken using Zeiss LSM880 confocal microscope, scale bar represents 50 μm .

GraphPad Prism version 5.01 (GraphPad Software, San Diego, USA).

Infection of HepG2/C3A spheroids with *P. falciparum* NF54

P. falciparum NF54 parasites were maintained in continuous culture using established method (Trager and Jensen, 1976). Sexual stages of the parasites were cultured at 4% haematocrit in complete medium (RPMI 1640 with L-glutamine, 25 mM HEPES pH 7.4 (Gibco), 2 g/L sodium bicarbonate, 50 mg/ml hypoxanthine (Sigma) and 10% human heat-inactivated AB + serum) from 0.5% mixed stage asexual cultures. Media was changed daily for 16–17 days and appearance of gametocyte stages was monitored every 48–72 h by microscopic analysis of thin blood smears (Delves *et al.*, 2016).

Female *Anopheles coluzzii* mosquitoes aged between 5 and 7 days were deprived of sugar for 18–20 h prior to infection. The standard membrane feeding assay was used to provide the mosquitoes with *P. falciparum* NF54 cultures containing stage V gametocytes for 30 min (Tripathi *et al.*, 2020). Afterwards, engorged mosquitoes were incubated in insectary conditions and offered ad libitum 10% sucrose solution. On day 16 post-infection with *P. falciparum* NF54, mosquitoes were collected and washed with 70% v/v ethanol and dissected to obtain salivary glands. Salivary glands were crushed in PBS and sporozoites stored in liquid nitrogen until required.

HepG2/C3A spheroids, grown as described above, were infected with *P. falciparum* NF54 20×10^4 sporozoites per spheroid and incubated at 37 °C with 5% CO₂. On day 4 post-infection,

HepG2/C3A spheroids were fixed with 4% paraformaldehyde for 1 h at 4 °C and liver stage parasites detected by immunofluorescent staining of *P. falciparum* GAPDH and HSP70, as described above. The percentage of infected hepatocytes was calculated semi-quantitatively by counting the number of GAPDH or HSP70 positively fluorescing cells and dividing by the total cell number, as visible from DAPI staining of representative images from 4 spheroids, from 2 experimental replicates. Media changes were performed every 48–72 h to maintain HepG2/C3A spheroids.

To access blood-stage breakthrough, human O+ erythrocytes were introduced to *P. falciparum* NF54 infected HepG2/C3A spheroids at a final haematocrit of 0.1% in complete EMEM and incubated at 37 °C, with 5% CO₂. On day 8 and day 12, 50 μL samples were taken from each well and gassed with 3% O₂, 4% CO₂ and 93% N₂ and replenished with EMEM and human erythrocytes. To monitor asexual stage development, thin blood smears were prepared from the blood samples and stained with 10% Giemsa. Slides were examined under oil immersion at 100 \times using a Zeiss LSM880 confocal microscope (Zeiss, Germany). A schematic of the timeline for infection and sample collection is shown in Figure 1.

Results

HepG2/C3A spheroid formation and spheroid structure

To confirm the reproducibility of HepG2/C3A spheroid generation, assays to characterize spheroid formation and liver-like functions were undertaken, prior to infection with *Plasmodium*, as reported previously (Gaskell *et al.*, 2016; Štampar *et al.*, 2020).

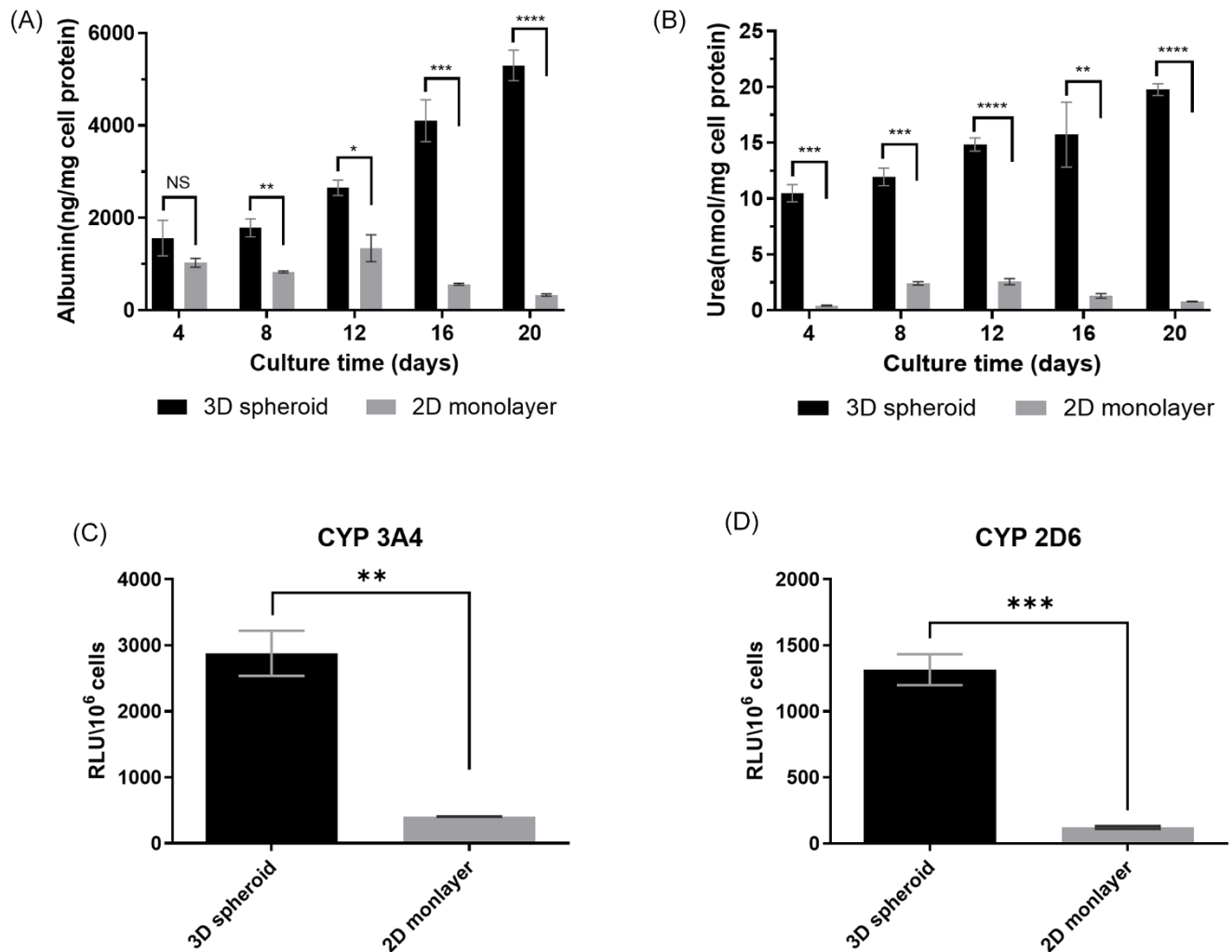


Figure 4. Functional characterization of HepG2 3D spheroids and 2D cultures. Quantification of (A) albumin and (B) urea from HepG2/C3A grown in 2D and as 3D spheroids supernatants, normalized by mg cell protein on days 4, 8, 12, 16 and 20. Data were analysed by multiple unpaired *t*-tests with Holm–Šidák correction for multiple comparisons. Comparison of (C) CYP 3A4 and (D) CYP 2D6 expression from HepG2/C3A grown in 2D and as 3D spheroids on day 4, normalized by cell number, expressed as relative light units (RLU) per 10⁶ cells. Data were analysed by unpaired *t*-test. All data represent the mean \pm SEM of 3 independent experiments, performed with 2 technical replicates. **p* < 0.05, ***p* < 0.01, ****p* < 0.001.

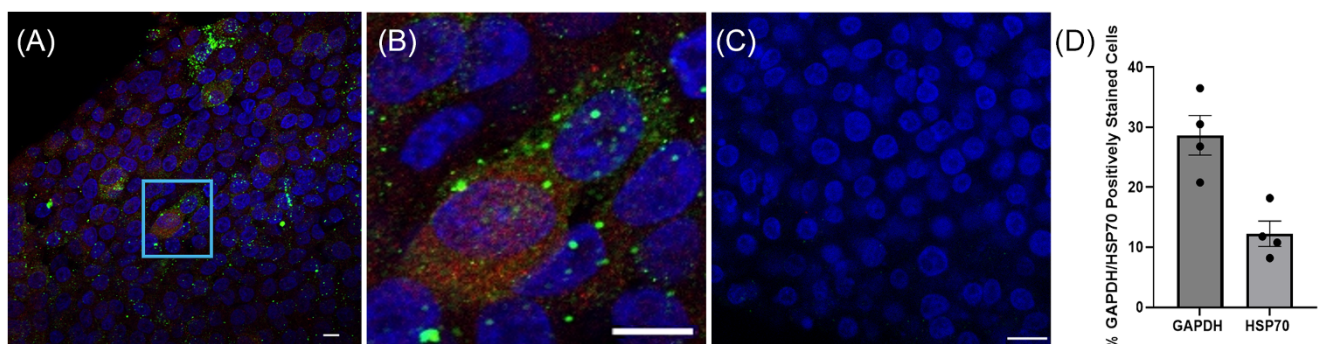
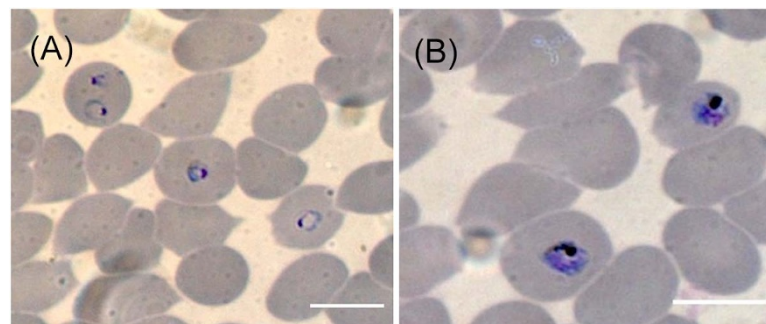


Figure 5. Assessment of HepG2/C3A 3D spheroid culture infection by *P. falciparum* NF54 sporozoites and asexual blood stage breakthrough from infected HepG2/C3A 3D spheroids. (A) Liver stage parasites were detected by immunofluorescence on day 4 post-infection and stained with antibodies towards GAPDH (green [monoclonal antibody 7.2 anti-GAPDH 1:100, obtained from the European Malaria Reagent Repository (<http://www.malariaearesearch.eu>)] and HSP70 (red [rabbit anti-HSP70 *P. falciparum* polyclonal, 1:200, StressMarq Biosciences Inc., SPC-186D]), cell nuclei are visualized with DAPI stain (blue). Region of interest (ROI) is shown in light blue box. (B) Close-up of ROI showing staining of GAPDH (green) and HSP70 (red) surrounding cell nuclei (blue). (C) Uninfected HepG2/C3A spheroid control. (D) Infection burden was expressed as the percentage of positively stained GAPDH or HSP70 hepatocytes relative to hepatocytes with no colocalized staining with DAPI. Data displayed are from *n* = 2 biological replicates, carried out in duplicate. Error bars represent SEM. Images were obtained with Zeiss LSM880 confocal microscope (Zeiss, Germany) white scale bar represents 10 μ m.

Figure 6. Asexual blood stage breakthrough from infected HepG2/C3A 3D spheroids. Human erythrocytes were introduced to infected HepG2/C3A cultures at a final haematocrit of 0.1% in complete EMEM and incubated for 6 days. Giemsa-stained thin blood films were performed on samples from day 8 and day 12 following infection with *P. falciparum* NF54 which were gassed with 3% O₂, 4% CO₂ and 93% N₂, $n = 5$ HepG2/C3A spheroids. On day 8 ring stage parasites were observed (A) and by day 12 trophozoite/early schizont parasites could also be detected (B). Slides were examined under oil immersion at 100 \times using a Zeiss LSM880 confocal microscope (Zeiss, Germany) white scale bar represents 10 μ m.



Spheroids aggregated by day 5 (Figure 2A) and their diameter increased between day 5 and day 21 from $210 \mu\text{m} \pm 6.07$ to $483.16 \mu\text{m} \pm 19.26$, respectively (Figure 2B). F-actin filaments and hepatocyte transporters (Pg-P and MRP2) were visualized by immunofluorescence staining on days 4 and 15. HepG2/C3A spheroid polarization was confirmed by colocalization of F-actin with Pg-P and MRP2 (Figure 3). 2D monolayer HepG2/C3A cells were also imaged on days 4 and 15 and although F-actin filaments were visible at both time points, MRP2 and Pg-P transporters were not observed (Figure 3).

Confirmation of liver-like function in spheroids

Spheroid albumin and urea production was quantified over 20 days and compared with 2D monolayers (Figure 4A, B). Albumin production in 2D monolayer cells remained low throughout the 20-day time course, with maximum albumin production observed on day 12 ($1343.77 \text{ ng/mg} \pm 290.77$ albumin). After day 12, albumin production in monolayer cells further reduced to $360.60 \text{ ng/mg} \pm 23.12$ by day 20. 3D spheroids, however, demonstrated increases in albumin levels throughout the 20-day period, with the greatest albumin production observed on day 20 ($5303.63 \text{ ng/mg} \pm 329.63$). Significantly more albumin was produced in 3D spheroids, compared to 2D monolayer cells from day 8 onwards (Figure 4A). Similarly to albumin, urea production in 2D monolayer cells peaked on day 12 ($2.58 \text{ nmol/mg} \pm 0.27$) and decreased afterwards to $0.784 \text{ nmol/mg} \pm 0.029$ by day 20. In contrast, 3D spheroid urea production increased over 20 days from $10.49 \text{ nmol/mg} \pm 0.77$ on day 4 to $19.77 \text{ nmol/mg} \pm 0.522$ on day 20. Significantly more urea was produced from 3D spheroids compared to 2D monolayer cells at every time point (Figure 4B).

To access liver metabolism in HepG2/C3A 3D and 2D cultures, CYP3A4 and CYP2D6 activity was measured. Both enzymes have significant roles in drug metabolism (Tornio and Backman, 2018; Zhao *et al.*, 2021) and would, therefore, be essential for any future works characterizing anti-malaria drug efficacy. CYP3A4 activity was 7-fold higher and CYP2D6 10-fold greater in 3D spheroids (Figure 4C; $2878 \pm 2.6 \text{ RLU/106 cells}$, $1315 \pm 2.0 \text{ RLU/106 cells}$, respectively) compared to 2D culture (Figure 4D; $405 \pm 0.7 \text{ RLU/106 cells}$, $122 \pm 1.03 \text{ RLU/106 cell}$, respectively).

HepG2/C3A spheroid infection with *P. falciparum* NF54 sporozoites and *Plasmodium* asexual blood-stage breakthrough from HepG2/C3A spheroids to human erythrocytes

Spheroids were grown for 5 days and infected with 20×10^4 *P. falciparum* NF54 sporozoites and incubated for a further 4 days, post-infection. Spheroids were then fixed and stained with antibodies to

the sporozoite liver stage proteins GAPDH and HSP70 to confirm the presence of *P. falciparum* infection during the exoerythrocytic (hepatic) stages (Figure 5A, B). Uninfected control spheroids did not show staining of GAPDH or HSP70 (Figure 5C). Infection burden of liver spheroids was quantified in a semi-quantitative manner counting GAPDH or HSP70 positive cells as a percentage of infected hepatocytes relative to uninfected hepatocytes from representative spheroid images (Figure 5D). GAPDH and HSP70 indicated an infection burden of $28.7\% \pm 3.3\%$ SEM and $12.3\% \pm 2.12\%$ SEM, respectively.

To access if HepG2/C3A infected spheroids were able to lead to blood-stage breakthrough, human erythrocytes were introduced on day 6, on 2 separate occasions and incubated till day 12. On day 8, a thin blood film was then prepared, and erythrocytes were observed to contain ring staged parasites (Figure 6A). After 12 days, another thin blood film was then prepared and trophozoite/early schizont parasites were seen (Figure 6B). Blood stage breakthrough was observed from all infected spheroids.

Discussion

The HepG2/C3A liver spheroid model developed here represents a low-cost, accessible means to explore the complete intrahepatic lifecycle of *P. falciparum*, addressing significant limitations faced by many laboratories in adopting advanced *in vitro* models for malaria research.

3D cell culture technologies have increasingly been recognized for their ability to more accurately model *in vivo* cellular behaviour *in vitro* relative to 2D cultures. The hepatocytes within the 3D-grown HepG2/C3A spheroid were shown to be structurally and functionally polarized, recapitulating the *in vivo* condition (Godoy *et al.*, 2013). Secondary structures composed of F-actin were observed forming enhanced networks throughout the spheroids, that were associated with Pg-P and MRP2, transporters localized to the canalicular membrane of hepatocytes, as described elsewhere (Gaskell *et al.*, 2016). HepG2/C3A spheroids displayed enhanced synthesis and secretion of liver proteins, albumin and urea, as well as enhanced CYP metabolism, as exemplified by raised CYP 3A4 and CYP 2D6 expression, compared to monolayer cultures. CYP 3A4 and CYP 2D6 expression was then shown to increase over time in 3D spheroids. It should be noted that CYP metabolism comparison between monolayer and 3D spheroids was conducted on day 4 only, as accurate comparisons could not be assured as the spheroid size and density grew and full penetration of CYP luciferin pro-substrates could not be guaranteed. This could, therefore, have led to an underestimation of differential CYP expression, compared to 2D monolayers. These data support previous observations (Gaskell *et al.*, 2016; Štampar *et al.*, 2020) and confirm that

cells cultured in 3D have superior functionality to those cultured in 2D (Cox *et al.*, 2020; Tutty *et al.*, 2022).

Previous attempts to create stable *in vitro* models of malaria life stages using immortalized hepatoma cell lines, such as HepG2, have had limited success and failed to demonstrate breakthrough infection into erythrocytes (Chattopadhyay *et al.*, 2010; Tweedell *et al.*, 2019; Valenciano *et al.*, 2022). However, the structural and functional attributes of 3D-grown HepG2/C3A cells appear to offer the necessary physiological conditions for *P. falciparum* intrahepatocytic development. Our findings suggest these conditions are essential for completing the parasite's lifecycle within hepatic cells.

The current study is limited as it is a qualitative assessment of blood-stage breakthrough from *P. falciparum* infected HepG2/C3A liver spheroids using a relatively large sporozoite infection burden. To fully benchmark this system against existing liver-stage models, a more extensive comparative study would be required in the future. The described HepG2/C3A 3D spheroids model also presents a unique opportunity to identify proteins involved in stage conversion in follow-on studies. These studies were beyond the scope of the presented article; however, one recent global gene expression study of human malaria parasite liver stages revealed significantly increased expression of genes in central metabolic pathways and redox homeostasis (Zanghi *et al.*, 2023). It is noteworthy that previous studies have shown that HepG2/C3A 3D spheroids replicate the liver's zonation due to oxygen and nutrient gradients (Gaskell *et al.*, 2016; Cox *et al.*, 2020). It will be important to determine whether the critical contributing factor to the permissiveness of the 3D spheroid model to intrahepatocytic parasite development is that the specific nutrient and redox needs of the parasite can be met by the unique spatiotemporal microenvironment of the spheroid.

In summary, the HepG2/C3A liver spheroid model lowers barriers to malaria research by offering a simpler and more accessible method to study the hepatic stages of *P. falciparum* infection. This model addresses a critical gap in malaria research tools and can significantly enhance our ability to study fundamental aspects of *Plasmodium* biology and develop effective liver-stage interventions. This approach not only broadens the scope of research possibilities but also provides a platform for high-throughput screening of antimalarial drugs and vaccines, promoting advancements in both fundamental biology and translational research.

Author contributions. CHC, SOA, AA, JC, AS, LR, DSE and JBJ conducted data gathering. CHC and SOA performed statistical analyses. SOA, AA, AS, LR, KJD, SHP, PS, SAW and GAB contributed to the study design. CHC, SOA and GAB wrote the article. GAB conceived the study.

Financial support. For the purpose of open access, the authors have applied a Creative Commons Attribution (CC BY) licence to any Author Accepted Manuscript version arising from this submission. This study was supported by funding from the Medical Research Council (MR/W002248/1, MR/L000644/1 and MR/R015678/1) and by the Bureau Culture of Saudi Arabia under the directives of King Salman Bin Abdulaziz (SOA).

Competing interests. The authors declare there are no conflicts of interest.

Ethical standards. Not applicable.

References

Chattopadhyay R, Velmurugan S, Chakiath C, Donkor LA, Milhous W, Barnwell JW, Collins WE and Hoffman SL (2010) Establishment of an *in vitro* assay for assessing the effects of drugs on the liver stages of *Plasmodium vivax* malaria. *PLoS ONE* 5, e14275. doi:10.1371/journal.pone.0014275

Cox CR, Lynch S, Goldring C and Sharma P (2020) Current perspective: 3D spheroid models utilizing human-based cells for investigating metabolism-dependent drug-induced liver injury. *Frontiers in Medical Technology* 2, 2673–3129. doi:10.3389/fmedt.2020.611913

Delves MJ, Straschil U, Ruecker A, Miguel-Blanco C, Marques S, Dufour AC, Baum J and Sinden RE (2016) Routine *in vitro* culture of *P. falciparum* gametocytes to evaluate novel transmission-blocking interventions. *Nature Protocols* 11, 1668–1680. doi:10.1038/nprot.2016.096

Gaskell H, Sharma P, Colley HE, Murdoch C, Williams DP and Webb SD (2016) Characterization of a functional C3A liver spheroid model. *Toxicology Research* 5, 1053–1065. doi:10.1039/c6tx00101g

Godoy P, Hewitt NJ, Albrecht U, Andersen ME, Ansari N, Bhattacharya S, Bode JG, Bolleyn J, Borner C, Böttger J, Braeuning A, Budinsky RA, Burkhardt B, Cameron NR, Camussi G, Cho CS, Choi YJ, Rowlands JC, Dahmen U, Damm G, Dirsch O, Donato MT, Dong J, Dooley S, Drasdo D, Eakins R, Ferreira KS, Fonsato V, Fraczek J, Gebhardt R, Gibson A, Glanemann M, Goldring CEP, Gómez-Lechón MJ, Groothuis GMM, Gustavsson L, Guyot C, Hallifax D, Hammad S, Hayward A, Häussinger D, Hellerbrand C, Hewitt P, Hoehme S, Holzhütter HG, Houston JB, Hrach J, Ito K, Jaeschke H, Keitel V, Kelm JM, Park BK, Kordes C, Kullak-Ublick GA, LeCluyse EL, Lu P, Luecke-Wheeler J, Lutz A, Maltman DJ, Matz-Soja M, McMullen P, Merfort I, Messner S, Meyer C, Mwinyi J, Naisbitt DJ, Nussler AK, Olinga P, Pampaloni F, Pi J, Pluta L, Przyborski SA, Ramachandran A, Rogiers V, Rowe C, Schelcher C, Schmich K, Schwarz M, Singh B, Stelzer EHK, Stieger B, Stöber R, Sugiyama Y, Tetta C, Thasler WE, Vanhaecke T, Vinken M, Weiss TS, Widera A, Woods CG, Xu JJ, Yarborough KM and Hengstler JG (2013) Recent advances in 2D and 3D *in vitro* systems using primary hepatocytes, alternative hepatocyte sources and non-parenchymal liver cells and their use in investigating mechanisms of hepatotoxicity, cell signaling and ADME. *Archives of Toxicology* 87, 1315–1530. doi:10.1007/s00204-013-1078-5

Maher SP, Vantaux A, Chaumeau V, Chua ACY, Cooper CA, Andolina C, Péneau J, Rouillier M, Rizopoulos Z, Phal S, Piv E, Vong C, Phen S, Chhin C, Tat B, Ouk S, Doeurek B, Kim S, Suriyakan S, Kittiphanakun P, Awuku NAA, Conway AJ, Jiang RHY, Russell B, Bifani P, Campo B, Nosten F, Witkowski B and Kyle DE (2021) Probing the distinct chemosensitivity of *Plasmodium vivax* liver stage parasites and demonstration of 8-aminoquinoline radical cure activity *in vitro*. *Scientific Reports* 11, 19905. doi:10.1038/s41598-021-99152-9

Roth A, Maher SP, Conway AJ, Ubalee R, Chaumeau V, Andolina C, Kaba SA, Vantaux A, Bakowski MA, Thomson-Luque R, Adapa SR, Singh N, Barnes SJ, Cooper CA, Rouillier M, McNamara CW, Mikolajczak SA, Sather N, Witkowski B, Campo B, Kappe SHI, Lanar DE, Nosten F, Davidson S, Jiang RHY, Kyle DE and Adams JH (2018) A comprehensive model for assessment of liver stage therapies targeting *Plasmodium vivax* and *Plasmodium falciparum*. *Nature Communications* 9, 1837. doi:10.1038/s41467-018-04221-9

Siqueira-Neto JL, Wicht KJ, Chibale K, Burrows JN, Fidock DA and Winzeler EA (2023) Antimalarial drug discovery: Progress and approaches. *Nature Reviews Drug Discovery* 22, 807–826. doi:10.1038/s41573-023-00772-9

Štampar M, Breznik B, Filipič M and Žegura B (2020) Characterization of *in vitro* 3D cell model developed from human hepatocellular carcinoma (HepG2) cell line. *Cells* 9, 2557. doi:10.3390/cells9122557

Tornio A and Backman JT (2018) Chapter one - Cytochrome P450 in pharmacogenetics: An update. In Brösen K and Damkier P (eds), *Advances in Pharmacology*. Academic Press, 3–32. doi:10.1016/bs.apha.2018.04.007

Trager W and Jensen JB (1976) Human malaria parasites in continuous culture. *Science* 193, 673–675. doi:10.1126/science.781840

Tripathi AK, Mlambo G, Kanatani S, Sennis P, and Dimopoulos G (2020) *Plasmodium falciparum* gametocyte culture and mosquito infection through artificial membrane feeding. *Journal of Visualized Experiments: JoVE* 161, e61426. doi:10.3791/61426

Tutty MA, Movia D and Prina-Mello A (2022) Three-dimensional (3D) liver cell models - A tool for bridging the gap between animal studies and clinical trials when screening liver accumulation and toxicity of nanobiomaterials. *Drug Delivery & Translational Research* 12, 2048–2074. doi:10.1007/s13346-022-01147-0

- Tweedell RE, Tao D, Hamerly T, Robinson TM, Larsen S, Grønning AGB, Norris AM, King JG, Law HCH, Baumbach J, Bergmann-Leitner ES and Dinglasan RR (2019) The selection of a hepatocyte cell line susceptible to *Plasmodium falciparum* sporozoite invasion that is associated with expression of glypican-3. *Frontiers in Microbiology* **10**. doi:[10.3389/fmicb.2019.00127](https://doi.org/10.3389/fmicb.2019.00127)
- Valenciano AL, Gomez-Lorenzo MG, Vega-Rodríguez J, Adams JH and Roth A (2022) In vitro models for human malaria: Targeting the liver stage. *Trends in Parasitology* **38**, 758–774. doi:[10.1016/j.pt.2022.05.014](https://doi.org/10.1016/j.pt.2022.05.014)
- World Malaria Report (2023) Geneva: World Health Organization; 2023. Licence: CC BY-NC-SA 3.0 IGO.
- Zanghi G, Patel H, Camargo N, Smith JL, Bae Y, Flannery EL, Chuenchob V, Fishbaugher ME, Mikolajczak SA, Roobsoong W, Sattabongkot J, Hayes K, Vaughan AM and Kappe SHI (2023) Global gene expression of human malaria parasite liver stages throughout intrahepatocytic development. *bioRxiv: The Preprint Server for Biology* 2023.01.05.522945. doi:[10.1101/2023.01.05.522945](https://doi.org/10.1101/2023.01.05.522945)
- Zhao M, Ma J, Li M, Zhang Y, Jiang B, Zhao X, Huai C, Shen L, Zhang N, He L and Qin S (2021) Cytochrome P450 enzymes and drug metabolism in humans. *International Journal of Molecular Sciences* **22**, 12808. doi:[10.3390/ijms222312808](https://doi.org/10.3390/ijms222312808)